Pergamon

Int. J. Heat Mass Transfer. Vol. 38, No. 9, pp. 1577–1585, 1995
Copyright © 1995 Elsevier Science Ltd
Printed in Great Britain. All rights reserved
0017-9310/95 $9.50+0.00

0017-9310(94)00276-2

Heat transfer in granular activated carbon beds in the presence of adsorbable gases

R. E. CRITOPH
Engineering Department, University of Warwick, Coventry CV4 7AL, U.K.

and

L. TURNER†
Rolls Royce Industrial and Marine Gas Turbine Division, Ansty, Coventry, U.K.

(*Received* 21 *January* 1994 *and in final form* 23 *August* 1994)

Abstract—The thermal conductivity of an active carbon bed in vacuum, helium, neon and argon has been measured at temperatures up to 200°C. A modified version of the Zehner–Bauer model is developed which successfully describes the results. The model is expanded to include the variation in grain conductivity due to the adsorbed phase when the bed is exposed to an adsorbable gas. The expanded model is verified by conductivity measurements with ammonia at up to 11.3 bar pressure and 25% mass concentration. Conductivities are predicted to +3.1%, −2.5%. Bed conductivities with ammonia are typically 0.165 W m^{-1} K^{-1}, with minor changes due to concentration, but the grain conductivity varies between 0.85 and 1.25 W m^{-1} K^{-1} as a non-linear function of concentration.

INTRODUCTION

The ability of activated carbons to adsorb large mass concentrations of refrigerant gases makes them ideal for use in heat driven (adsorption) refrigeration and heat pump systems [1]. In the process of heating a granular bed of active carbon above ambient temperature (desorbing refrigerant) and then cooling it back to ambient temperature (adsorbing refrigerant), a thermodynamic cycle is performed which results in refrigeration or heat pumping as required. In order to make these systems economically viable, their size (and inventory of adsorbent and refrigerant) must be reduced [2]. This implies a need for rapid heating and cooling of the adsorbent bed to improve the power output per mass of carbon. Granular beds tend to be poor conductors and so there is a need both to understand the heat and mass transfer within the bed and to improve on it.

The favoured combinations of adsorbent and refrigerant are active carbon with methanol or ammonia [1, 3], zeolites with water or ammonia [4], or chemical adsorbents such as calcium chloride with ammonia [5]. Heat transfer in carbon–methanol beds has been studied by Guilleminot and Meunier and others [6, 7], zeolite–water beds by Sahnoune and Grenier [8], and salt–ammonia beds by Mauran *et al.* [9]. This study investigates the thermal conductivity of carbon–ammonia beds. Sutcliffe–Speakman's coconut shell activated carbon 208C was chosen for its good adsorptive properties with ammonia and was used throughout the experimental programme.

THEORY OF HEAT TRANSFER IN PACKED GRANULAR BEDS

Early models utilized an idealized geometry, for which the temperature field could be solved using the Fourier law. The usefulness of this approach was limited since there are only a few configurations for which there are closed form solutions and they are not particularly realistic. More general models based on Ohm's law were developed to relate the bed porosity ψ, the grain or solid conductivity λ_s and the gas conductivity λ to the overall bed conductivity λ_{so}. Models assume either parallel isotherms perpendicular to the heat flux (zero lateral resistance) or heat flux uniform in the direction of heat transfer (infinite lateral resistance). These provide bounds to the real solution. Unit cell geometries vary; including hyperbolic shaped grains, lamellae and touching spheres [10–13]. The major problems associated with theses models are unrealistic assumptions regarding heat flow and particle array geometries. Zehner [14] introduced a variable contour particle shape and assumed parallel heat flux lines, as shown in Fig. 1. Bauer [15] extended the work and the Zehner–Bauer model is the most extensive and complete of its kind. The unit cell consists of a solid central core, a mixed bed region and

† Formerly at the University of Warwick.

NOMENCLATURE

A	relative area of solid conduction path within grain
B	deformation factor
C_s	modified Stephan–Boltzmann constant = 5.67
K	constant in Dubinin–Astakhov equation
n	exponent in Dubinin–Astakhov equation
p	term defined in equation (4)
r	radius of the solid core in the Zehner–Bauer model unit cell
T	temperature (K)
x	mass concentration
x_0	maximum mass concentration
x_R	effective radiation length of the particle packing
Z	height in the Zehner–Bauer model unit cell.

Greek symbols

ε	emissivity of the solid surface
λ	thermal conductivity (of gas unless subscripted)
ϕ	relative area of grain to grain contact
ψ	porosity (pore volume/bed volume)
ψ_g	grain porosity (micropore volume/grain volume).

Subscripts

ad	adsorbed phase
b	overall bed
b*	effective mixed bed
g	solid grain without micropores
R	radiation
s	solid grain
s*	solid grain with adsorbed phase
sat	saturation.

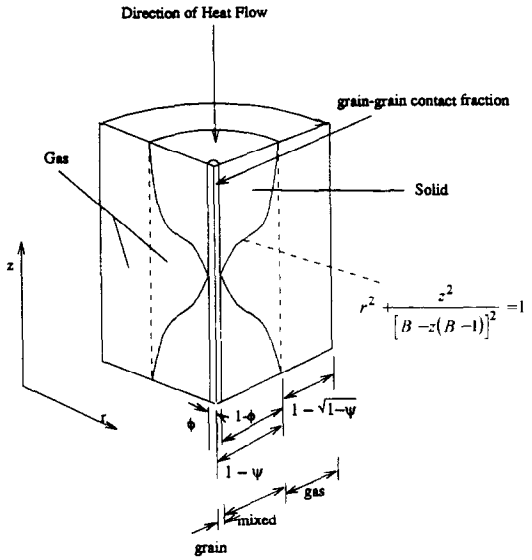

Fig. 1. The Zehner–Bauer model.

an outer annulus of gas. It has unit volume, height and cross-sectional area. The shape of the solid core is generated using equation (1):

$$r^2 + \frac{z^2}{[B-z(B-1)]^2} = 1. \quad (1)$$

The deformation factor B allows the solid core to have a range of shapes from a thin cylinder when $B = 0$, a sphere when $B = 1$ and a thick cylinder when $B \to \infty$. It is by virtue of this extra degree of freedom that the Zehner–Bauer model generally produces a superior fit to experimental results. This is because the errors introduced into the equation by assuming uniform geometry and parallel heat flux may be minimized by distorting the particle geometry to fit the result. The unit cell particle shape is not necessarily similar to that of the real particle. Six possible heat transfer mechanisms are modelled:

(1) conduction through the grain;

(2) conduction from grain to grain through an area of contact;

(3) conduction through the gas phase;

(4) conduction through the gas phase near points of contact where the mean free path of the gas molecules is comparable to the volume in which they move (Knudsen effect);

(5) radiant heat transfer from grain to grain;

(6) radiant heat transfer from void to void.

There are three material phases in the unit cell which transfer heat along parallel flux lines. These are a solid volume, a gas volume and the remaining mixed volume which is part solid and part gas. A full discussion and derivation of the model is given by Turner [16]. The resulting equations are complex but explicit functions of bed properties. A simplification made here is that the Knudsen effect on gas conductivity is negligible at the likely operating pressures and temperatures of an ammonia–carbon refrigerator or heat pump. This is justified in the results section. The simplified Zehner–Bauer equations are:

$$\frac{\lambda_b}{\lambda} = \{1-\sqrt{1-\psi}\}\left[1+\psi\frac{\lambda_R}{\lambda}\right] + \sqrt{1-\psi}\left(\phi\frac{\lambda_s}{\lambda}\right) + \sqrt{1-\psi}(1-\phi)\frac{\lambda_{b^*}}{\lambda} \quad (2)$$

$$\frac{\lambda_{b^*}}{\lambda} = \frac{2}{p}\left[\frac{B\frac{\lambda}{\lambda_s}\left(\frac{\lambda_s}{\lambda}+\frac{\lambda_R}{\lambda}-1\right)}{p^2}\ln\left(\frac{\frac{\lambda_s}{\lambda}+\frac{\lambda_R}{\lambda}}{B}\right) - \frac{B-1}{p}+\frac{B+1}{2B}\frac{\lambda_R}{\lambda}\right]-B \quad (3)$$

$$p = 1+\frac{\lambda}{\lambda_s}\left(\frac{\lambda_R}{\lambda}-B\right). \quad (4)$$

The radiation conductivity λ_R is given by equation (5), which is based on radiation exchange between two parallel surfaces with a modification to allow for the non-parallel nature of the pore shape and for the use of the pore depth as a characteristic dimension:

$$\frac{\lambda_R}{\lambda} = \frac{0.04C_s}{\lambda(2/\varepsilon-1)}\left(\frac{T}{100}\right)^3 x_R. \quad (5)$$

The equations are derived in full by Turner in ref. [16]. There are four unknowns in the above equations which relate to the bed (rather than gas) properties:

B which describes the cell geometry

ϕ the relative grain–grain contact area

$\frac{x_R}{2/\varepsilon-1}$ the effective radiation length and emissivity

λ_s the grain conductivity.

When a gas is adsorbed within the micropores of the adsorbent grain, it is expected that λ_s will change. The standard Zehner–Bauer model does not allow for this effect and must be modified accordingly. The quantitative effect is described and interpreted in later sections.

THERMAL CONDUCTIVITY MEASUREMENTS

A steady-state method of measurement was adopted to avoid any mass transfer effects that might occur due to desorption in transient heating. The test equipment is unique in that all other such measurements in the literature are low pressure devices. This equipment is designed to withstand pressures up to 30 bar and temperatures up to 200°C with an ammonia–carbon pair. The test vessel takes the form of a 316L stainless steel annular container for the carbon bed, as shown in Fig. 2. Temperature conditions in the bed are determined by three pairs of electric heaters on the outer wall and against the inner wall. The upper and lower pairs are guard heaters and the central heater is used for measurement. The inner heaters are powered by a low voltage d.c. amplifier controlled by computer and using a PID algorithm to maintain a set temperature. They take the form of high resistance (7 $\Omega\,m^{-1}$) heating wire in glass fibre sleeving wrapped on a glass tube which fits tightly into the steel vessel's inner tube. Electrical connection to the heating wires

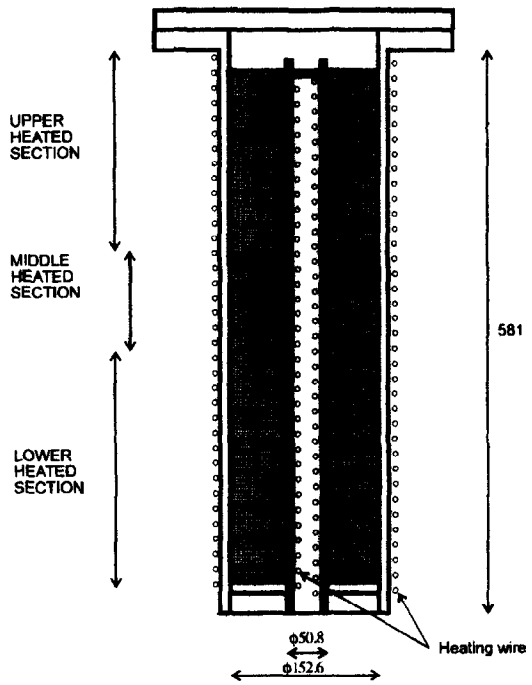

Fig. 2. Test vessel.

was via silver soldered copper wires which passed through holes drilled in the glass tube and out through the inside of the glass tube, which was packed with mineral fibre insulation. Five K-type thermocouples were mounted on the three inner heaters with only their junctions exposed on the tube surface, the cable being lead away in the same fashion as the power cables. The central (measurement) temperature is measured by a single thermocouple, whilst the temperature differences between the centre heater and the upper and lower guard heaters are measured by pairs of back-to-back mounted thermocouples. When the whole vessel is in a steady state, the heat loss through the measuring annulus is the heat generated in the inner central heater, which is calculated from the voltage measured across it.

The outer three heaters use identical wire and sleeving to the inner heaters wound on a 2 mm pitch on the outside of the vessel. The outer heaters are powered from the 240 V a.c. supply via thyristor controllers. The heater's function is not just to control the outside temperature, but to provide the bulk of the energy required to raise the mass of the vessel to the required temperature. Each heater temperature is measured by a bare ended thermocouple fixed to the pressure vessel wall. The temperature measurements are made by a PID algorithm in the computer software to maintain the desired constant level. For tests where the temperature exceeds 90°C, a ceramic fibre insulating jacket is placed around the vessel. At lower temperatures a thin layer of 'kaowool' is sufficient.

In addition to the six cylindrical heaters it was found necessary to use top and bottom end heaters, each with a separate thyristor controller. Without the end

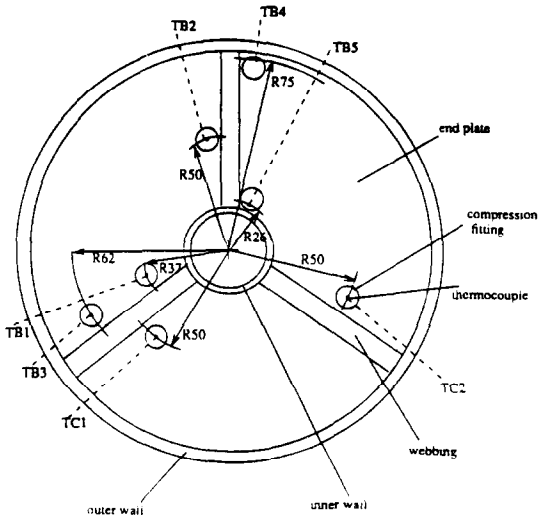

Fig. 3. Position of thermocouples.

plate heaters it was found that longitudinal heat losses occurred along the cylindrical steel walls.

The temperature profile across the bed was measured by seven stainless steel sheathed K-type thermocouples with a diameter of 1 mm. It was found by the use of a finite difference model that the distance between their centres should not be less than 12 mm to ensure that the thermocouples themselves did not provide paths of enhanced conductance. Figure 3 shows their positions. TB4 and TB5 are positioned 1 mm from the outer and inner bed walls, respectively. TB2, TC1 and TC2 are all positioned half-way between the inner and outer bed radii. TC1 and TC2 are used to check the accuracy of the thermocouple positioning and it was found that all three thermocouples agreed within a 0.5°C band. TB1 and TB3 are placed one quarter and three quarters of the way between the inner and outer radii, respectively.

Before use the carbon must be degassed. The vessel is heated to 200°C whilst connected to a rotary vacuum pump producing 0.1 torr for 24 h. A diffusion pump is then used to complete the degassing process with a further 24 h at 10^{-4} torr. The carbon is stored in an argon atmosphere when not in use, since argon is effectively non-adsorbable. When the conductivity of the bed is measured with ammonia it is necessary to control the system pressure as well as the temperature. The vessel is connected to an ammonia reservoir of 1.6 l volume, which is immersed in a temperature-controlled oil bath. There is sufficient ammonia in the system to ensure that there is always liquid in the reservoir and so the ammonia pressure is always the saturation pressure corresponding to the temperature in the oil bath. Since fixing both pressure and temperature determines the concentration of the ammonia in the carbon, conductivity can be measured at any desired level of concentration.

In use it may take 48 h for the vessel to reach a steady state. It is judged that steady state has been reached when the voltage to the inner heater does not vary by more than ± 0.01 V for a continuous 15 h.

The power to the inner heater is used to calculate the bed thermal conductivity on the assumption that there is one-dimensional radial heat transfer. An error analysis for the temperature, position, voltage and resistance measurements reveals that the accuracy of the power measurement is $\pm 2.0\%$, giving an accuracy of the overall bed conductivity of $\pm 6.1\%$. One further source of inaccuracy in the results must be overcome. Longitudinal heat leakage between the middle heater and the guard heaters might occur, due to the possibility of heater thermocouples being placed on either hot or cold spots. This problem is overcome by making two measurements of each overall bed conductivity, with different temperature differences across the bed but all other parameters identical. Plotting the power against the temperature difference and extrapolating the line to find the power for zero temperature difference reveals the longitudinal heat flux which is deducted from the total to give the radial flux. Initial experiments with four data points revealed the power–temperature difference relationship to be linear, as anticipated, and only two points are needed in practice. The longitudinal heat loss from the central heater varied from 0.4 to 0.06 W as the temperature of the bed ranged from 230 to 35°C. This was typically 3–7% of the power measured at the highest temperature difference.

TEST PROGRAMME

Before thermal conductivity tests were carried out a number of preliminary tests on the carbon were needed to provide data on the porosity:

(1) The total void volume (inter particle space plus the volume of macropores, mesopores and micropores) was measured using helium pressurization of the vessel containing the carbon. The pressure and temperature are measured before and after the vessel is opened to a second evacuated vessel of known volume. The initial volume occupied by the helium is easily calculated and can be compared with the volume of the carbon vessel. Since helium is assumed not to be adsorbed the total void volume is obtained. The ratio of void volume to total volume for the bed used is 0.77.

(2) The inter granular void volume is measured by filling all micro-, macro- and mesopores with water. After soaking in water (which results in vigorous expulsion of air from the grains), the outsides of the grains are dried by blowing ambient-temperature air over the separated grains until they are dry to the touch. In order to check that the grains are still as full as possible with water, the immersion and drying process is repeated, but it is assumed that the grains were in fact full, since no further gas is evolved from the grains. The carbon is packed into a measuring cylinder which is large enough to ensure that packing

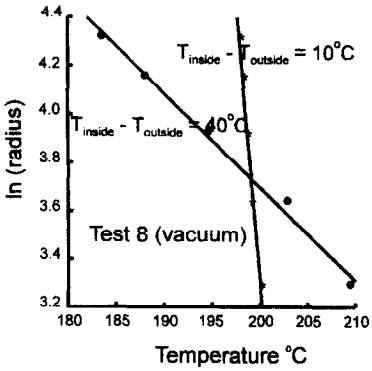

Fig. 4. Bed temperature vs ln (radius) for test 8.

distortion at the edge is negligible. The carbon is packed to a level marker of predetermined volume and the mass of the beaker and contents is weighed. Water is then added up to the level marker and the beaker reweighed. The difference enables the inter granular void volume ψ to be calculated. For the bed used ψ is 0.478.

(3) The adsorption characteristics of the carbon ammonia pair used were measured using techniques described by Critoph and Turner [17]. A modified Dubinin–Astakhov equation relates concentration x, temperature T and pressure, as defined by the saturation temperature T_{sat} of the gas:

$$x = x_0 \exp\left[-K\left(\frac{T}{T_{sat}} - 1\right)^n\right]. \quad (6)$$

For the 208C carbon:

$$x_0 = 0.2582$$

$$K = 3.984$$

$$n = 1.305.$$

The thermal conductivity tests were carried out in pairs, as described above. Since the heat flux is radial, a plot of the logarithm of radius against the temperature of the five thermocouples in the bed is linear and the slope of the line together with the power gives the bed conductivity. Each set of data points was fitted to a straight line with a range of standard estimates of error of 0.1–3.0%, as illustrated by Fig. 4 and shown in full by Table 1. A total of 19 tests are presented; four under vacuum, six with helium, three with argon, one with neon and five with ammonia. The results are analysed in the following section.

ANALYSIS OF RESULTS USING THE ZEHNER–BAUER MODEL

The results of helium tests 1 and 2 are highly significant when using the Zehner–Bauer model to represent high pressure systems. The mean measured conductivity for both is 0.664 W m^{-1} K^{-1}, despite conditions which minimize and maximize the mean free path expected in an ammonia–carbon refrigerator or heat pump. This implies that the neglect of the Knudsen effect on gas conductivity is justified in this case. This is not so with low-pressure systems such as carbon–methanol [7] or zeolite–water [8].

The results for vacuum, helium and argon are used to find the four unknown parameters from the Zehner–Bauer model. This is checked against the result for neon in order to give a degree of confidence in the method and then, with all parameters but the grain conductivity fixed, the ammonia results are analysed to give grain conductivity as a function of ammonia concentration.

A specially written MATLAB routine is used to minimize the differences between measurements and theory for the four parameters. More data points than measured are required by the routine, and these are derived by fitting three quadratic equations to the data for vacuum, helium and argon at different temperatures. It has already been established that there is no pressure effect and the fit is very good, as seen in Fig. 5.

The routine is used to determine best fit values for the four unknowns, minimizing three possible functions:

$$\sqrt{\sum_{n=0}^{i} (\lambda_{so}\text{measured} - \lambda_{so}\text{generated})^2} \quad (7a)$$

$$\sum_{n=0}^{i} (\lambda_{so}\text{measured} - \lambda_{so}\text{generated})^2 \quad (7b)$$

$$\sum_{n=0}^{i} (\lambda_{so}\text{measured} - \lambda_{so}\text{generated})^4. \quad (7c)$$

These generate mean errors of 3.2%, 3.4% and 5.0%, respectively, but are biased towards low (vacuum), medium (argon) and high (helium) bed conductivities, respectively. Since the gas conductivities of argon and ammonia are similar, the parameters generated by equation (7b) were used with the ammonia data. The fit is illustrated in Fig. 6 and the parameters are:

$$B \quad 1.3764$$

$$\phi \quad 0.02959$$

$$\frac{x_R}{2/\varepsilon - 1} \quad 0.00293$$

$$\lambda_s \quad 0.9738.$$

These values, when used to predict the one measurement with neon, give an error of 5.6%, which is considered acceptable compared with the experimental error.

It is useful to consider the physical significance of the model parameters. ϕ and B define the particle geometry. The relative solid–solid contact area ϕ is low. This is to be expected since examination under the microscope of a section of bed potted in resin shows little contact.

The deformation factor B is 1.3764, which means that the apparent shape of the particle is nearly that

Table 1. Measured bed conductivities in vacuum, helium, neon, argon and ammonia

Test no.	Medium	Mean temperature [K]	Pressure [bar]	SEE [%]	λ_b [W m^{-1} K^{-1}]	Mean λ_b [W m^{-1} K^{-1}]
1	Helium	510.4	30	0.29	0.660	0.664
				0.13	0.667	
2	Helium	510.5	3.7	0.31	0.656	0.664
				0.18	0.672	
3	Helium	436.6	1.0	0.29	0.512	0.517
				0.13	0.521	
4	Helium	380.8	1.0	0.77	0.428	0.425
				0.24	0.422	
5	Argon	381.0	1.0	1.14	0.170	0.169
				0.30	0.168	
6	Argon	426.5	1.0	0.70	0.190	0.191
				0.11	0.192	
7	Argon	481.5	1.0	0.34	0.231	0.233
				0.06	0.235	
8	Vacuum	470.8	0	1.26	0.106	0.108
				0.06	0.109	
9	Vacuum	420.8	0	2.07	0.081	0.082
				0.07	0.082	
10	Vacuum	370.3	0	3.30	0.065	0.065
				0.43	0.065	
11	Helium	380.8	1.0	0.77	0.442	0.439
				0.31	0.436	
12	Ammonia	312.1	1.56	1.94	0.165	0.163
				1.23	0.160	
13	Ammonia	311.7	4.24	2.83	0.168	0.165
				1.60	0.162	
14	Ammonia	312.0	5.79	1.52	0.172	0.171
				1.47	0.170	
15	Ammonia	312.1	7.00	1.08	0.171	0.173
				1.41	0.174	
16	Ammonia	312.0	11.30	1.05	0.191	0.187
				1.20	0.186	
17	Vacuum	312.7	0	1.41	0.047	0.047
				3.90	0.047	
18	Neon	312.0	1.0	0.93	0.214	0.217
				1.24	0.219	
19	Helium	312.0	1.0	0.98	0.358	0.361
				1.03	0.363	

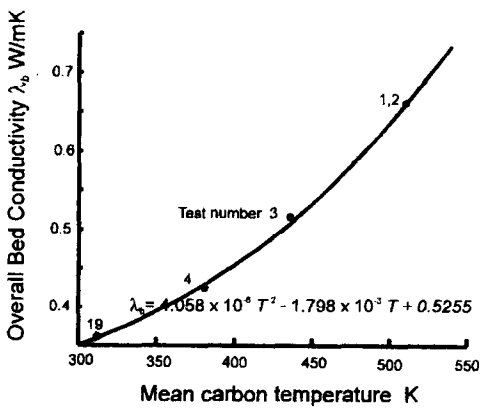

Fig. 5. A quadratic curve fitted to the bed conductivity in helium vs temperature.

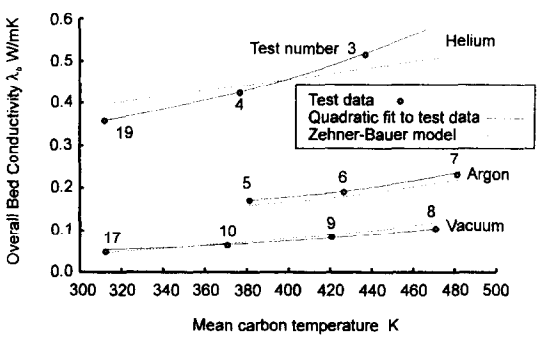

Fig. 6. Comparison of experimental data and model.

of a sphere. This is reasonable with the knowledge that ψ, the inter granular void ratio, is 0.478.

The radiation term is 0.00293. It is estimated that the emissivity of a black glassy body is about 0.8 [19]. If this is the case, then x_R is 4.4 mm. This term characterizes the effective radiation path length of the particle packing. Again, by observation of a section, the gap size is seen to vary from 0 to 8 mm and so the value found is quite reasonable.

Lastly, consider the grain conductivity. Unlike the other three parameters, this is a true property rather than an effective characteristic. The value of λ_s in this case is 0.874 W m^{-1} K^{-1} and this compares well with

Table 2. Bed and grain conductivities under varying ammonia concentration

Test no.	Mean temperature [K]	Pressure [bar]	Concentration [kg kg^{-1}]	λ_b [W m^{-1} K^{-1}]	λ_{s^*} [W m^{-1} K^{-1}]
12	312.1	1.56	0.133	0.163	0.850
13	311.7	4.24	0.188	0.165	0.875
14	312.0	5.79	0.207	0.171	0.963
15	312.1	7.00	0.218	0.173	0.994
16	312.0	11.30	0.245	0.187	1.250
Calculated	313.0	n.a.	0	0.863	0.863

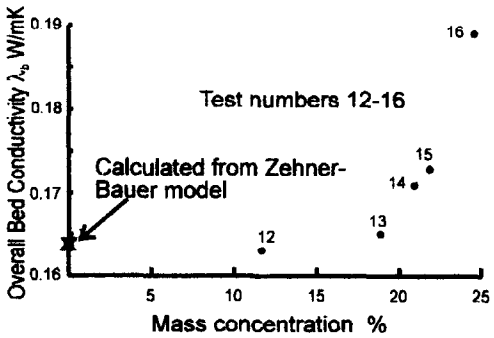

Fig. 7. Bed conductivity vs ammonia concentration.

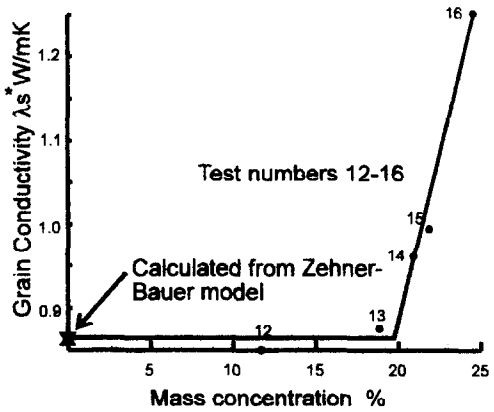

Fig. 8. Grain conductivity vs ammonia concentration.

other quoted values. Hayashi *et al.* [20] derived a value of 0.651 W m^{-1} K^{-1} for the grain conductivity of an unnamed active carbon. Gurgel and Grenier [7] derived a value of 0.54 W m^{-1} K^{-1} using the Zehner–Bauer model for the grain conductivity of AC35, a coal-based extruded active carbon. It is expected that different active carbons will vary in conductivity. The grain may be considered to consist of disordered graphitic platelets with holes or pores burnt into them. The more intact the matrix the better the conductivity, or, conversely, the higher the porosity the lower the conductivity.

The measurements in the presence of ammonia are used to investigate the effect of adsorbed ammonia on the grain conductivity, now a variable λ_{s^*}. Table 2 shows the test results, together with the ammonia concentration calculated from equation (6) and the grain conductivity calculated from the Zehner–Bauer model. In addition, the model is used to predict the hypothetical case of ammonia being present but not adsorbed. This provides a zero concentration point in Figs. 7 and 8, which show the variation of bed and grain conductivity with concentration.

MODELLING GRAIN CONDUCTIVITY

Figure 9 shows the physical process of adsorption by micropore filling. It shows a slit-shaped micropore within the grain. As ammonia is adsorbed it firstly forms a single layer of molecules over the inner surface of the pore (monolayer adsorption). On an increase in pressure or reduction in temperature, further layers of adsorbed ammonia build up until eventually they

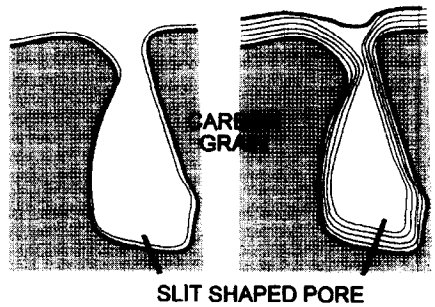

Fig. 9. Physical process of micropore filling.

combine to form a meniscus at the narrowest cross-section of the pore.

When considering a whole grain, heat may be transferred by two mechanisms only. Firstly there is conduction along solid paths uninterrupted by pores. Secondly there is conduction through the grain and empty, partially filled or completely filled pores. When the micropore is empty, it can be assumed that its conductivity is negligible compared to that of the grain material. This is because the micropores are so small (2–50 nm) that the radiation conductivity is of the order 10^{-9} W m^{-1} K^{-1} and gas conduction is dominated by the Knudsen effect. This means that when the pore is empty heat transfer is only by the first mechanism.

When the pores are full, heat transfer is by both mechanisms and can be modelled by the unit cell pro-

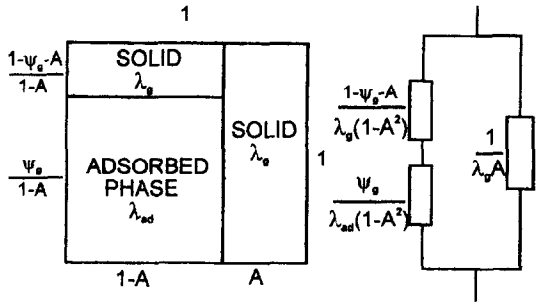

Fig. 10. Grain unit cell.

posed in Fig. 10. The conductivity of the grain is found from the overall resistance of the network:

$$\lambda_{s^*} = \lambda_g A + \frac{\lambda_g \lambda_{ad}(1-A)^2}{\lambda_{ad}(1-\psi_g - A) + \psi_g \lambda_g}. \quad (8)$$

In the case of zero concentration the equation reduces to:

$$\lambda_{s^* x=0} = \lambda_g A. \quad (9)$$

The adsorbate conductivity and density can be assumed to be that of the liquid phase [18], the micropore volume ratio ψ_g is known and overall grain conductivity λ_{s^*} has been measured for a maximum concentration (micropores full) and calculated for zero concentration. Solving these equations gives a value of 0.333 for A and 2.59 W m^{-1} K^{-1} for λ_g. To confirm the value of the thermal conductivity of the grain solid material would require further tests with other adsorbates to give a good range of values of overall grain conductivity. However Gurgel and Grenier [7] obtained a value of 1.06 W m^{-1} K^{-1} for the AC-35 methanol pair and so the value for 208C is not unreasonable given that it is not an extruded carbon.

Figure 7 shows that the overall grain conductivity can be represented as two intersecting straight lines. This reflects the fact that micropore filling takes place in two stages. Firstly, the layers of adsorbent build up on the inner walls of the pore. This does not affect the thermal conductivity of the grain, since there is still an insulating gap in the centre of the pore. This stage is represented by the horizontal line.

The second phase of pore filling is the joining together of the adsorbed phase layers to form menisci in the throats of the pores. This is accompanied by a rise in the grain conductivity due to the establishment of a continuous path for heat transfer. This is represented by the sloping line. Quantitatively the results are represented by:

$$\lambda_{s^*} = 0.8625 \quad 0 \leqslant x \leqslant 0.1973$$

$$\lambda_{s^*} = 0.07866x - 0.6885 \quad 0.1973 < x \leqslant 0.2582. \quad (10)$$

Test 16 indicates a particularly high, possibly anomolous, grain conductivity. Natural convection effects at the high pressure are excluded because the logarithmic radial temperature distribution typical of conduction is maintained. The temperature distribution also negates the possibility of large variations in conductivity within the bed, but it is possible that very close to saturation there are other factors which might enhance the conductivity.

It is difficult to present a model which would be true for any activated carbon. Gurgel and Grenier [7] do not observe the two phases of pore filling when using AC35. They observe a linear increase in λ_{s^*} over the whole concentration range. Sahnoune and Grenier [8] do observe the two phases with zeolite NaX and water. It is suggested that λ_{s^*} reflects the uniformity of pore size. If there is a wide pore size distribution, as for AC35, then some pores will become full at nearly all concentrations and contribute to a change in conductivity. When the pore sizes fall within a narrow band, the point of sudden increase in the conductivity is very definite. This is suggested as the mechanism present in the case of carbon 208C.

Since λ_{s^*} is so dependent on the pore size distribution, then without detailed knowledge of the individual carbon it is impossible to present a general model for the grain. It would not be unreasonable however to use an average value for the bed conductivity over the whole concentration range. The mean value for λ_b is 0.1725 W m^{-1} K^{-1} and this gives the conductivity of the packed granular bed including the adsorbed phase with an accuracy of $\pm 7.1\%$.

Acknowledgement—Sutcliffe Speakman plc for the supply of active carbons.

REFERENCES

1. F. Meunier, La sorption solide: une alternative aux CFC's, *Proceedings of Solid Sorption Refrigeration*, pp. 44–52. International Institute of Refrigeration, Paris (1992).
2. R. E. Critoph, Refrigeration in developing countries—the renewable options, *Proceedings of the World Renewable Energy Congress*, pp. 761–766. Pergamon Press, Oxford (1990).
3. D. J. Miles, D. M. Sanborn, G. A. Nowakowski and S. V. Shelton, Gas fired sorption heat pump development, *Proceedings of Solid Sorption Refrigeration*, pp. 74–79. International Institute of Refrigeration, Paris (1992).
4. G. Restuccia, V. Recupero, G. Cacciola and M. Rothmeyer, Zeolite heat pump for domestic heating, *Energy* **13**, 333–342 (1988).
5. B. Spinner, Les transformateurs thermochimiques à ammoniac, *Proceedings of Solid Sorption Refrigeration*, pp. 145–152. International Institute of Refrigeration, Paris (1992).
6. J. J. Guilleminot and F. Meunier, Heat and mass transfer in a non-isothermal fixed bed solid adsorbent reactor: a uniform pressure—non-uniform temperature case, *Int. J. Heat Mass Transfer* **30**, 1595–1606 (1987).
7. J. M. Gurgel and Ph. Grenier, Mesure de la conductivité thermique du charbon actif AC-35 en présence de gaz, *Chem. Engng J.* **44**, 43–50 (1990).
8. H. Sahnoune and Ph. Grenier, Mesure de la conductivité thermique d'une zeolithe, *Chem. Engng J.* **40**, 45–54 (1989).
9. S. Mauran, P. Prades and F. L'Haridon, Transferts de chaleur et de masse en milieux réactifs consolidés pour

systèmes thermochimiques, *Proceedings of Solid Sorption Refrigeration*, pp. 239–244. International Institute of Refrigeration, Paris (1992).
10. R. A. Crane and R. I. Vachon, A prediction of the bounds on the effective thermal conductivity of granular materials, *Int. J. Heat Mass Transfer* **20,** 711–722 (1977).
11. R. G. Deissler and J. S. Boegli, An investigation of the effective thermal conductivities of powders in various gases, *Trans. ASME* **8,** 1417–1425 (1958).
12. N. Wakao and K. Kato, Effective thermal conductivity of packed beds, *J. Chem. Engng Jap.* **2,** 23–33 (1969).
13. T. E. Schumann and V. Voss, Heat flow through granulated materials, *Fuel* **13,** 249–256 (1934).
14. P. Zehner, Experimentelle und theoretische Bestimmung der effectiven Warmeleitfahrigekeit Durchstromter Kugelschuttungen bei massigen und hohen Temperaturen, Dipl. Ing. thesis, University of Karlsruhe (1972).
15. R. Bauer, Effective radiale Warmleitfahrigekeit Gasdurchstomter Schuttungen mit Partikeln unterschiedlicher Form und Grossenverteilung, *VDI Forschungsh.* **582** (1977).
16. L. Turner, Improvement of activated charcoal–ammonia adsorption heat pumping/refrigeration cycles. Investigation of porosity and heat/mass transfer characteristics, Ph.D. thesis, University of Warwick (1992).
17. R. E. Critoph and L. Turner, Performance of ammonia-activated carbon and ammonia–zeolite heat pump adsorption cycles, *Proceedings of Pompes à Chaleur Chimiques de Hautes Performances*, pp. 202–211. Lavoisier, Paris (1988).
18. M. Smisek and S. Cerny, *Active Carbon Manufacture, Properties and Applications*. Elsevier, New York (1970).
19. Touloukian and De Witt, Thermal radiative properties of non-metallic solids, *Thermophysical Properties of Matter*. TPRC Series 8. IFI Plenum, New York (1970).
20. S. Hayashi *et al.*, A theoretical model for the estimation of the effective thermal conductivity of a packed bed of fine particles, *Chem. Engng J.* **35,** 51–60 (1987).